

Advances in quantum teleportation

S. Pirandola^{1*}, J. Eisert², C. Weedbrook³, A. Furusawa⁴ and S. L. Braunstein¹

Quantum teleportation is one of the most important protocols in quantum information. By exploiting the physical resource of entanglement, quantum teleportation serves as a key primitive across a variety of quantum information tasks and represents an important building block for quantum technologies, with a pivotal role in the continuing progress of quantum communication, quantum computing and quantum networks. Here we summarize the basic theoretical ideas behind quantum teleportation and its variant protocols. We focus on the main experiments, together with the technical advantages and disadvantages associated with the use of the various technologies, from photonic qubits and optical modes to atomic ensembles, trapped atoms and solid-state systems. After analysing the current state-of-the-art, we finish by discussing open issues, challenges and potential future implementations.

It has been over two decades since the discovery of quantum teleportation, in what is arguably one of the most interesting and exciting implications of the ‘weirdness’ of quantum mechanics. Prior to this landmark discovery, the fascinating idea of teleportation belonged in the realm of science fiction. First coined in 1931 by Charles H. Fort¹, the term ‘teleportation’ has since been used to refer to the process by which bodies and objects are transferred from one location to another, without actually making the journey along the way. Since then it has become a fixture of pop culture, perhaps best exemplified by Star Trek’s celebrated catchphrase “Beam me up, Scotty.”

In 1993, a seminal paper² described a quantum information protocol, dubbed quantum teleportation, that shares several of the above features. In this protocol, an unknown quantum state of a physical system is measured and subsequently reconstructed or ‘reassembled’ at a remote location (the physical constituents of the original system remain at the sending location). This process requires classical communication and excludes superluminal communication. Most importantly, it requires the resource of quantum entanglement^{3,4}. Indeed, quantum teleportation can be seen as the protocol in quantum information that most clearly demonstrates the character of quantum entanglement as a resource: without its presence, such a quantum state transfer would not be possible within the laws of quantum mechanics.

Quantum teleportation plays an active role in the progress of quantum information science^{5–8}. On the one hand, it is a conceptual protocol that is crucial in the development of formal quantum information theory; on the other, it represents a fundamental ingredient to the development of many quantum technologies. Quantum repeaters⁹, quantum gate teleportation¹⁰, measurement-based quantum computing¹¹ and port-based teleportation¹² all derive from the basic scheme of quantum teleportation. The vision of a quantum network¹³ draws inspiration from this scheme. Teleportation has also been used as a simple tool for exploring ‘extreme’ physics, such as closed time-like curves¹⁴.

Today, quantum teleportation has been achieved in laboratories around the world using a variety of different substrates and technologies, including photonic qubits (light polarization^{15–21}, single rail^{22,23}, dual rails^{24,25}, time-bin^{26–28} and spin-orbital qubits²⁹), nuclear magnetic resonance (NMR)³⁰, optical modes^{31–39}, atomic ensembles^{40–43},

trapped atoms^{44–48} and solid-state systems^{49–52}. Outstanding achievements have been made in terms of teleportation distance^{20,21}, with satellite-based implementations forthcoming. Attempts at scaling to more complex quantum systems have also begun²⁹.

Basics of quantum teleportation

We start by reviewing the basic quantum teleportation protocol in both finite- and infinite-dimensional settings.

Quantum teleportation of qubits and discrete variables. Quantum teleportation was originally described for two-level quantum systems, which are referred to as qubits². The protocol considers two remote parties — Alice and Bob — who share two qubits, A and B , prepared in a pure entangled state. In the ideal case, this is taken to be maximally entangled, such as $|\Phi\rangle = (|0,0\rangle + |1,1\rangle)/\sqrt{2}$ (known as a Bell pair⁵). At the input, Alice is given another qubit a whose state ρ is unknown. She then performs a joint quantum measurement, called Bell detection^{53–55}, which projects her qubits a and A into one of the four Bell states $(\mathcal{P}_k \otimes I)|\Phi\rangle$ with $k = 0, 1, 2, 3$, where $\mathcal{P}_k \in \{I, X, Z, ZX\}$ is a Pauli operator^{5,6} (X is the bit-flip operator and Z is the phase-flip operator). As a result, the state of Alice’s input qubit has been collapsed by measurement while Bob’s qubit B is simultaneously projected onto $\mathcal{P}_k^\dagger \rho \mathcal{P}_k$. In the last (feed-forward) step of the protocol, Alice communicates the classical outcome k of her measurement to Bob, who then applies \mathcal{P}_k to recover the original input state ρ .

Note that Alice’s input state is assumed to be unknown, otherwise the protocol reduces to remote state preparation⁵⁶. Furthermore, this state may itself be part of a larger composite quantum system that is shared with a third party (in which case, successful teleportation requires reproducing all correlations with that third party). In typical experiments, the input state is taken to be pure and belonging to a limited alphabet, for example, the six poles of the Bloch sphere⁵ or another unbiased sample of states. In the presence of decoherence, the quality of the reconstructed state may be quantified by its teleportation fidelity $F \in [0, 1]$. This is the fidelity⁵ between Alice’s input state and Bob’s output state, averaged over all the outcomes of the Bell detection and input state alphabet. For small values of the fidelity, strategies exist that allow for an imperfect teleportation while making no use of any entangled resource. For example, Alice

¹Computer Science and York Centre for Quantum Technologies, University of York, York YO10 5GH, United Kingdom. ²Dahlem Center for Complex Quantum Systems, Freie Universität Berlin, 14195 Berlin, Germany. ³Department of Physics, University of Toronto, Toronto M5S 3G4, Canada. ⁴Department of Applied Physics, The University of Tokyo, 7-3-1 Hongo, Bunkyo-ku, Tokyo 113-8656, Japan. *e-mail: stefano.pirandola@york.ac.uk

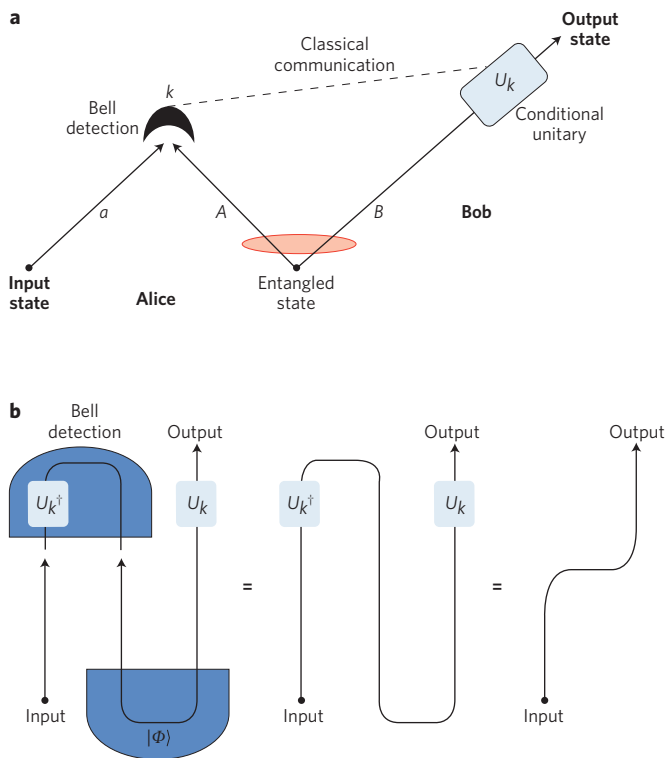


Figure 1 | Theory of quantum teleportation. **a**, Basic protocol. Alice's unknown input state is teleported to Bob using a shared entangled state and a classical communication channel. Alice performs a Bell state measurement on her systems, a and A , and classically communicates the outcome k to Bob. Using the measurement result, Bob applies the conditional unitary U_k to his system B , thus retrieving an output state that is an exact replica of Alice's input state in the ideal case ($F = 1$). The outcomes of the Bell detection are $k = 0, \dots, d^2 - 1$ for DV systems, and k is a complex number for CV systems. In qubit-teleportation ($d = 2$), the input state is typically pure, the entangled state is a Bell pair, and U_k is a qubit Pauli operator \mathcal{P}_k . In CV teleportation ($d = \infty$), the systems are bosonic modes (for example, optical), the input is typically a coherent state, the entangled state is an EPR state, and U_k is a phase-space displacement. Variations on this basic protocol may occur depending on the actual technologies adopted. **b**, Ideal teleportation process in terms of Penrose-inspired space-time diagrams¹³⁴. Let us consider a maximally entangled state $|\Phi\rangle$ as a shared quantum resource (that is, a Bell pair for qubits, or an ideal EPR state for CVs). The Bell detection then corresponds to applying $\langle\Phi|(U_k^\dagger \otimes I)$, where the outcome k is randomly selected by the measurement. As a result, an arbitrary input state ρ is transformed into $U_k^\dagger \rho U_k$ where the unitary U_k^\dagger is correspondingly 'undone' by Bob.

may directly measure her input state, thereby sending the results to Bob for him to prepare an output state⁵⁷. Such a measure-prepare strategy is known as 'classical teleportation' and has the maximum fidelity⁵⁸ $F_{\text{class}} = 2/3$ for an arbitrary input qubit state or, equivalently, an alphabet of mutually unbiased states, such as the six poles of the Bloch sphere. Thus, the requirement $F > F_{\text{class}}$ is a clear benchmark for ensuring that quantum resources are utilized.

Quantum teleportation is not restricted only to qubits, and may involve higher-dimensional quantum systems. One can formulate ideal teleportation schemes for every finite dimension d : this exploits a basis of maximally entangled states and a basis $\{U_k\}$ of unitary operators satisfying⁵⁹ $\text{tr}(U_j^\dagger U_k) = d\delta_{jk}$. The scheme then follows the above lines, with the Pauli operators \mathcal{P}_k replaced by U_k and the classical channel involves distinguishing d^2 signals. Such a protocol can be constructed for any finite-dimensional Hilbert space, for so-called discrete-variable (DV) systems (Fig. 1).

Quantum teleportation of continuous variables. Quantum teleportation can also be extended to quantum systems that have an infinite-dimensional Hilbert space, known as continuous-variable (CV) systems. These are typically realized by optical bosonic modes, whose electric field can be described by position- and momentum-like quadrature operators^{7,8}. Following the first theoretical proposals^{60,61}, CV teleportation was demonstrated with optical modes³¹. Other CV systems can be considered, including optomechanical systems⁶² and collective spins of atomic ensembles^{40,41}.

In the standard CV protocol with optical modes, the entangled resource corresponds to a two-mode squeezed vacuum state⁸, also known as an Einstein-Podolsky-Rosen (EPR) state. This is a zero-mean Gaussian state⁷ whose entanglement can be quantified in terms of the logarithmic negativity⁶³⁻⁶⁵ as $\max\{0, -\log_2 \epsilon\}$, where $\epsilon \geq 0$ can be computed from the covariance matrix⁷. Suppose Alice is given an input mode a in an unknown state; typically, a coherent state $|\alpha\rangle$ with unknown amplitude α . She then applies a CV Bell measurement on her modes, a and A , which consists of mixing them on a balanced beamsplitter and measuring the output ports with two homodyne detectors⁶⁶. This realizes the projection onto the quadratures $\hat{q}_- = (\hat{q}_a - \hat{q}_A)/\sqrt{2}$ and $\hat{p}_+ = (\hat{p}_a + \hat{p}_A)/\sqrt{2}$. In the last step, Alice communicates the classical outcome $k = q_- + ip_+$ to Bob, who performs a conditional displacement on his mode B (Fig. 1).

The teleportation fidelity for the alphabet of coherent states is given by $F = (1 + \epsilon)^{-1}$. Perfect teleportation occurs only for unbounded entanglement $\epsilon \rightarrow 0$, where the entangled state approximates the ideal EPR state, thus giving the perfect correlations $\hat{q}_A = \hat{q}_B$ and $\hat{p}_A = -\hat{p}_B$. Without entanglement ($\epsilon = 1$) we have $F = F_{\text{class}} = 1/2$; that is, the classical threshold for teleporting coherent states^{67,68}. A more stringent threshold asks that the teleported state is the best copy of the input allowed by the no-cloning bound⁶⁹, requiring $F > 2/3$. Note that this basic CV protocol can be extended to more general Gaussian state settings⁷⁰, for which suitable fidelity benchmarks can be derived⁷¹⁻⁷⁴. Finally, CV teleportation can also go broadband⁷⁵.

Variants of teleportation

Teleportation is an important primitive that has been extended in a number of ways. Some of these extensions are actual protocols of quantum technology, whereas others are of conceptual value in theoretical models. In this section, we mention some of these variants and outline some of the most recent developments.

Entanglement swapping and quantum repeaters. As previously mentioned, the input to be teleported can itself be part of an entangled state; teleportation would then also transfer the entanglement. When the Bell detection is performed by a third party, say Charlie acting as a middle relay, this variant is called entanglement swapping. Suppose that Alice and Bob do not share entanglement, but instead locally prepare two entangled states; ρ_{aA} at Alice's station and ρ_{bB} at Bob's. They retain systems a and b , while sending systems A and B to Charlie for Bell detection. After the measurement outcome k has been classically broadcast, Alice and Bob share the conditional output state $\rho_{ab|k}$, which is entangled. This can be implemented with DV systems⁷⁶ (for example, polarization qubits⁷⁷), CV systems⁷⁸⁻⁸¹ (for example, optical modes^{34,82}) or adopting a hybrid approach that involves both DVs and CVs⁸³.

This protocol forms the basis of a quantum repeater⁹, in which the combination of entanglement swapping and distillation^{84,85} allows for the distribution of entanglement over large distances. Once that maximal entanglement has been distilled along a long chain of repeaters, teleportation between the end-users provides the perfect transfer of quantum information. The remote correlations created by swapping can also be exploited in quantum cryptography: even when Charlie is present in the role of an eavesdropper (untrusted relay), Alice and Bob can transform their resulting correlations into a secret key^{86,87}.

Quantum teleportation networks. Another important extension is to a quantum teleportation network, where $n > 2$ parties share a multipartite entangled state to allow teleportation between any two parties. For simplicity, we describe the simplest case of a three-party network, where, for example, Alice can teleport to either Bob or Charlie. One simple strategy is known as assisted teleportation, whereby Charlie performs a local measurement on his system and broadcasts the result with the aim of improving the fidelity of quantum teleportation from Alice to Bob. This requires Charlie's operation to be tailored so as to increase the bipartite entanglement of the remaining parties.

With qubits, three-party assisted networks can be constructed using the Greenberger–Horne–Zeilinger state⁸⁸. In particular, this state makes teleportation equivalent to quantum secret sharing⁸⁹, whereby Alice's quantum information can be recovered by Bob if and only if Charlie assists. With CV systems, three-party assisted networks can be constructed with Gaussian states⁷⁰ generated, for example, using squeezed vacua at the input of two beamsplitters⁹⁰, as used in the first experimental demonstrations^{91,92}. In general, by using one or more squeezed vacua in an interferometer, one can create multiparty assisted networks that involve an arbitrary number of bosonic modes^{8,90}.

A second strategy is unassisted teleportation, whereby Charlie, rather than helping Alice, also receives a copy of the input. In this case, the protocol corresponds to quantum telecloning, with Alice teleporting to Bob and Charlie simultaneously, though with a teleportation fidelity limited by the no-cloning bound (5/6 for qubits^{93,94} and 2/3 for coherent states of CV systems⁹⁵). Quantum telecloning, from one sender to two recipients, has been experimentally implemented with polarized photonic qubits⁹⁶ and coherent states of optical modes⁹⁷. Theoretically, the protocol can be formulated for an arbitrary number of recipients, both in the case of qubits⁹⁸ and CV systems⁹⁹.

Quantum gate teleportation and quantum computing. Quantum teleportation can be expressed in terms of primitive quantum computational operations¹⁰⁰, and its protocol can be extended to quantum gate teleportation^{10,101}. This idea is rooted in the observation that unitary state manipulation can be achieved by preparing auxiliary entangled states, performing local measurements and applying single-qubit operations. This approach is at the heart of linear-optical quantum computing¹⁰² and plays an important role in fault-tolerant quantum computation. Essentially, certain gates are prepared offline as the entanglement resource for a teleportation protocol⁵. This resource is then also easier to implement in a fault-tolerant manner. Experimentally, two-qubit gates have been teleported¹⁰³.

More generally, such gate teleportation strategies lie at the heart of cluster-state quantum computing¹¹ and other schemes for measurement-based quantum computing¹⁰⁴. In these schemes, a number of nodes (qubits or qumodes⁷) are prepared in a multipartite entangled state (for example, a cluster state) or other suitable tensor network state. Then, a suitable measurement on one node teleports its state onto another node with the concurrent application of a desired quantum gate^{11,105}. Large cluster states can be generated with CV systems^{106,107}, with one experiment employing more than 10^4 optical modes¹⁰⁸.

Port-based teleportation. In port-based teleportation^{12,109}, Alice and Bob share n Bell pairs, which are referred to as ports. Alice then performs a suitable joint measurement on her n qubits and the system to be teleported, then communicates the outcome $k = 1, \dots, n$ to Bob. Finally, Bob discards all his systems except qubit k , which will be in the unknown state of Alice's input. Compared with conventional teleportation, port-based teleportation has the advantage that Bob does not need to apply a correction at the end of the protocol. The disadvantage, however, is that the teleportation fidelity approaches unity only in the limit of large n .

This scheme has limited practical applications owing to the large entanglement resources needed (although this can be improved by entanglement recycling¹¹⁰), but has significant importance for conceptual studies in quantum information theory. This approach is an important primitive for devising programmable quantum processors¹² that can store a unitary transformation and then apply it to an arbitrary state. It has also been used in ideas of instantaneous non-local quantum computation¹¹¹, in attacking schemes of position-based cryptography¹¹¹, and in assessments of communication complexity tasks. In fact, advantages in quantum communication complexity have generally been linked to violations of Bell inequalities, with port-based teleportation being the main proof tool¹¹².

Experimental status and challenges

We now discuss the main experimental achievements and challenges of quantum teleportation. Ideally, an experiment of quantum teleportation is successful when the following basic requirements are met:

- (1) The input state is arbitrary (within a suitable alphabet).
- (2) A third party, say Victor, supplies the input state to Alice and independently verifies Bob's output state (for example, through quantum state tomography or fidelity estimation).
- (3) Alice performs a complete Bell detection, which allows her to distinguish an entire basis of entangled states.
- (4) Bob applies conditional unitaries in real-time before Victor's verification (active feed-forward).
- (5) Teleportation fidelity exceeds the appropriate threshold, which is achievable by classical measure–prepare strategies.

In the laboratory, some of these conditions may not be met. In particular, the failure of condition (3) has led to probabilistic teleportation, wherein only a subset of the Bell states are accessible. In this case, the protocol has an associated Bell-efficiency that provides an upper bound to its overall success probability. For contrast, if condition (3) can be met, one can in principle perform deterministic teleportation.

Another critical condition is the realization of active (or real-time) feed-forward, whereby the outcomes of the Bell measurement are communicated in real-time to Bob and the conditional unitaries are actively performed on the output state, before being verified by Victor. This qualifies a teleportation experiment as 'active'. In 'passive' experiments, the feed-forward is either not implemented (for example, in those with 25% Bell-efficiency) or simulated in post-processing (that is, the unitaries are numerically applied during the tomographic reconstruction of the output). It is clear that the most complete teleportation experiments are those that are both deterministic and active.

Photonic qubits. The practical realization of a complete Bell detection is still a major issue for photonic qubits, as the simplest use of linear optics and photodetection allows at most two of the four Bell states to be distinguished^{53–55} — a Bell-efficiency limit of 50%. In principle, using linear optics and n ancillary qubits allows a single qubit to be teleported with better Bell-efficiencies¹⁰², approaching 100% for infinite n . This theoretical possibility clearly implies an overhead of quantum resources that is a non-trivial experimental challenge. Solving this problem is an active area of research^{113–115}.

The Innsbruck experiment¹⁵ probabilistically teleported a polarization qubit at a Bell-efficiency of 25%, with a later demonstration achieving 50% in a 600 m fibre-optic implementation across the river Danube¹⁶. One point¹¹⁶ about the Innsbruck experiment is that, because its implementation required Bob's teleported qubit to be detected, condition (2) above was rendered problematic. One might argue that this experiment achieved teleportation as a post-diction, which might earn it the term^{116,117} 'a posteriori teleportation'.

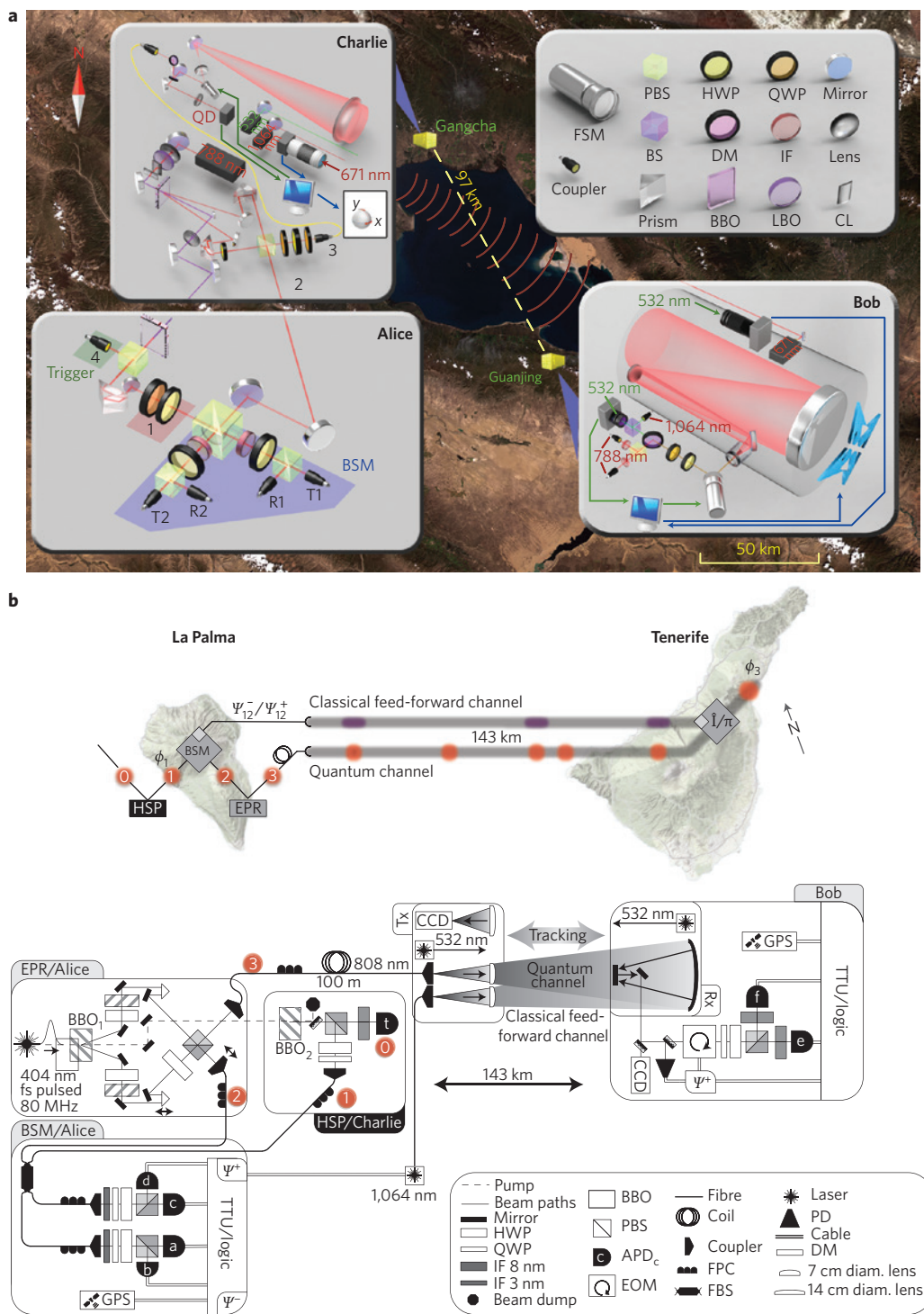


Figure 2 | Long-distance quantum teleportation with polarization qubits. **a**, A free-space, ground-level link measuring ~100 km across the Qinghai lake in China²⁰. Passive teleportation was implemented with 50% Bell-efficiency and 80% fidelity. The channel attenuation between Alice and Bob varied in the range of 35–53 dB. Besides atmospheric loss, major attenuation came from the beam spreading wider than the 40 cm aperture of the receiver telescope. The experiment relied on a point-and-track control system for the telescopes to compensate for atmospheric turbulence and ground settlement. Entanglement distribution over two ~50 km links (total loss of ~80 dB) was also implemented. T1, T2, R1 and R2 are detectors. BSM, Bell-state measurement; FSM, fast steering mirror; PBS, polarizing beamsplitter; BS, beamsplitter; HWP, half-waveplate; QWP, quarter-waveplate; DM, dichroic mirror; IF, interference filter; BBO, beta-barium borate; LBO, lithium triborate; CL, cylindrical lenses. **b**, A free-space link measuring 143 km at an altitude of 2,400 m between the Canary islands of La Palma and Tenerife²¹. Teleportation was implemented with 50% Bell-efficiency and a fidelity of 86% (for passive teleportation) and 83% (for active teleportation). A telescope with 1 m aperture was used at Bob's site, and the total channel attenuation varied in the range of 28–39 dB. The experiment involved a suitable tracking system and techniques to enhance the signal-to-noise ratio, including low-noise single-photon detectors with large active areas and entanglement-assisted clock synchronization. HSP, heralded single photon; Tx, transmitter; Rx, receiver; TTU, transistor-transistor unit; APD, avalanche photodiode; FPC, fibre polarization controller; FBS, fibre beamsplitter; PD, photodiode. All other acronyms as defined in **a**. Figures adapted with permission from: **a**, ref. 20, NPG; **b**, ref. 21, NPG.

To achieve complete Bell detection, the Rome experiment¹⁷ entangled photons in both spatial and polarization degrees of freedom. The input state was prepared within the set-up over one of the entangled photons, thus losing the ability to teleport entangled or mixed states. This implies that the input state cannot be independently supplied from outside, which violates condition (2) above. The scheme was later extended to free-space teleportation over 16 km at a fidelity of 89%¹⁸. Complete Bell detection has also been attempted using nonlinear interactions, although this leads to a very inefficient protocol. Using optical upconversion¹⁹, only one out of $\sim 10^{10}$ polarization qubits takes part in the nonlinear process.

Photonic qubits have also been physically realized in other ways. One is the single-rail qubit, or vacuum-one photon qubit¹¹⁸, which corresponds to the two-dimensional subspace spanned by the vacuum and the one-photon state of an optical mode. Such a qubit was teleported²² with 50% Bell efficiency and 95% fidelity. This implementation was later extended to real-time feed-forward with slightly reduced fidelity ($\sim 90\%$) in the first active experiment with photonic qubits²³. A direct generalization is the dual-rail qubit, which is a single photon encoded in one of two spatially separated modes¹⁰². This was teleported with 25% Bell efficiency and 80% fidelity by exploiting single photons generated by a quantum dot²⁴.

A photonic qubit has also been realized as a time-bin qubit¹¹⁹, which is a single photon populating one of two temporal modes. Time-bin qubits have been teleported along a 2 km spool of telecommunications fibre with 25% Bell-efficiency and 81% fidelity²⁶. The qubit was teleported between photons of different wavelengths (1.3–1.55 μm). This experiment was then extended to a relay configuration²⁷, where the Bell detection was performed by a third party, connected with Alice's input state and the entangled source by means of 2 km of coiled fibres. In this set-up, the challenge was to preserve the indistinguishability of the photons involved in the Bell detection. See ref. 28 for an implementation in a commercial telecommunications network.

Photonic qubits are excellent carriers for long-distance quantum communication. This is particularly true in free space, where birefringence is weak and photon absorption is small at optical frequencies (for example, compared with fibres). Two experiments with polarization qubits in free space^{20,21} achieved very long distance quantum teleportation. This suggests that the atmosphere can be traversed, placing satellite-to-ground implementations within reach of current technology (Fig. 2).

A complementary challenge is the photonic miniaturization of teleportation for applications in quantum processors based on linear optics and probabilistic gates¹⁰². Dual-rail qubits have been teleported within a photonic chip²⁵. Bell detection was performed with an efficiency of 1/27, and a fidelity of 89% was extrapolated by simulating the feed-forward operations in the post-processing. Active feed-forward remains a major challenge in photonic chips owing to the need for ultrafast photon detection and integrated electronics with terahertz bandwidths.

Finally, we have witnessed the (probabilistic and passive) teleportation of multiple degrees of freedom of a composite quantum system. The spin (polarization) and orbital angular momentum of a single photon have been teleported simultaneously²⁹, with a fidelity in the range of 57–68%. This is above the classical threshold of 40% given by the optimal state estimation for a single copy of a two-qubit system. The experiment exploited a hyper-entangled Bell detection with an efficiency of 1/32. The Bell detection was designed to be a quantum non-demolition measurement involving an additional teleportation set-up.

Nuclear magnetic resonance. Complete Bell detection is achievable in NMR teleportation³⁰, where the qubits are nuclear spins. The spins of two carbon nuclei (C_1 and C_2) and a hydrogen nucleus (H) were considered in a molecule of labelled trichloroethylene (more

precisely, an ensemble of such molecules, so that the results are averaged). After creating entanglement between C_1 and H through spin–spin interactions, teleportation was realized from C_2 to H by making a complete Bell detection on the two Carbon nuclei³⁰. This detection was performed in two steps¹⁰⁰: the Bell basis was first rotated to the computational basis using radiofrequency pulses and a spin–spin coupling; then, a projection on this basis was performed by exploiting the natural phase decoherence of the carbon nuclei (the fastest in the molecule, with times < 0.4 s). Real-time feed-forward was easily implemented using radiofrequency pulses. Because NMR teleportation is limited to inter-atomic distances, it is not suitable for quantum communication, but could still be used as a subroutine for NMR quantum computing.

Optical modes. The first and simplest resolution of the Bell detection problem came from the use of CV systems — in particular, optical modes³¹. As mentioned previously, the CV version of this measurement can easily be implemented with linear optics, using a balanced beamsplitter followed by two conjugate homodyne detections at the output ports. Both the beamsplitter visibility and the homodyne quantum efficiency can be extremely high, so that the overall detection can approach 100% efficiency. CV teleportation satisfies all conditions (1)–(5), the only restriction being that the input states must belong to a specific alphabet, as a consequence of the infinite-dimensionality of the Hilbert space. Real-time feed-forward can easily be implemented using electro-optical modulators (EOMs). The first experiment with optical modes³¹ was indeed deterministic and active, and successfully teleported an alphabet of fixed-energy phase-modulated coherent states with 58% fidelity — above the relevant classical threshold.

This experiment was later improved to beat the no-cloning bound, reaching fidelities of 70%³⁴ and 76%³⁵. These high-fidelity CV teleporters are able to transfer non-classical features such as non-positive Wigner functions. Other experiments with coherent states involved phase scanning at different amplitudes (61% fidelity³³) and simultaneous amplitude and phase modulation (64% fidelity³²). Other types of states have been teleported, including squeezed states^{35,36}, Schrödinger cat states³⁷ and entangled states (see entanglement swapping^{34,82,83}). Figure 3 shows typical experimental set-ups.

Unfortunately, CV teleportation fidelities cannot reach 100% because CV systems do not allow a maximally entangled state to be prepared with finite resources. Realistic EPR states, with good but finite two-mode squeezing, can be realized using a single, non-degenerate optical parametric oscillator^{120,121}. Alternatively, one can first produce two single-mode squeezed states, for example via parametric downconversion in two degenerate optical parametric oscillators, and then combine them in a balanced beamsplitter. Even with the high levels of squeezing currently feasible (~ 10 dB) this resource also requires good phase-locking in a teleportation experiment. The current fidelity record³⁸ for CVs is 83%.

To overcome the limitations due to finite squeezing, CV teleportation has been ‘integrated’ with DVs into a hybrid formulation^{122,123}. Deterministic and active CV teleportation of a photonic qubit has been realized³⁹ by applying a broadband CV teleporter to the temporal modes of a time-bin qubit. Such an approach aims to solve the problem of a complete Bell detection (thanks to CVs) while achieving a high teleportation fidelity thanks to DVs. Using only moderate levels of squeezing, one can achieve fidelities beyond 80% (Fig. 3b).

Optical modes are well-suited for integration into communication technologies, thanks to the use of high-performance homodyne detectors and off-the-shelf parts, like the EOMs used for the state input preparation and output displacements. Although it is unclear whether the CV teleportation distance is limited only to middle-range distances due to increased fragility with respect to loss (all previous experiments have been table-top), the possibility to go broadband and achieve high-rates is clearly appealing.

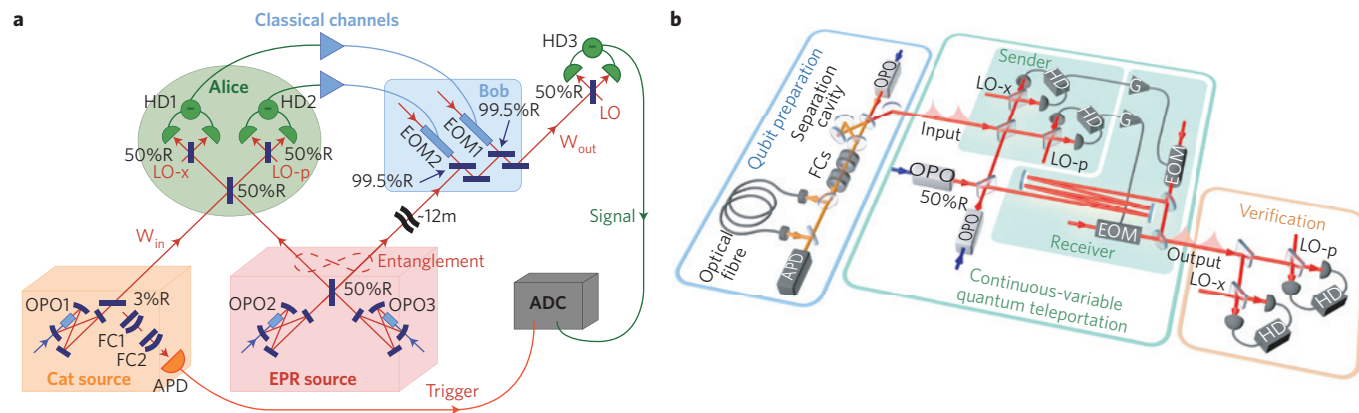


Figure 3 | Quantum teleportation with optical modes. **a**, Set-up of a full CV teleportation experiment with optical modes³⁷. An EPR state is generated by using two degenerate optical parametric oscillators (OPOs) and a balanced beamsplitter. At Alice’s station, part of the EPR state is combined with the input state (here a cat state) in a CV Bell detection; that is, another balanced beamsplitter with two homodyne detectors at the output ports. The classical outcomes are transmitted to Bob who displaces his part of the EPR state by using two EOMs. Note that both the preparation of the input state and the verification of the output state are independently done by Victor. ADC, analog-to-digital converter; R, reflectivity; FC, filter cavity; HD, homodyne detector; LO, local oscillator; LO-x, local oscillator locked at x-quadrature; LO-p, local oscillator locked at p-quadrature. **b**, Hybrid experiment where a time-bin qubit (prepared on the left) is teleported via CV teleportation (green middle section), involving an EPR state, complete CV Bell detection and EOMs³⁹. G, gain. All other acronyms as defined in **a**. Figures adapted with permission from: **a**, ref. 37, AAAS; **b**, ref. 39, NPG.

Atomic ensembles. Quantum teleportation may be performed between quantum systems of a different nature, for example, between light and matter. The first experiment to show this feature⁴⁰ involved teleporting coherent states of an optical mode onto the collective spin of an atomic ensemble comprising $\sim 10^{12}$ room-temperature caesium atoms. Because the collective transverse atomic spin components can be described by quadrature operators, this scheme implements a CV teleportation scheme.

Light-matter entanglement was generated by sending a strong light pulse through Bob’s atomic sample⁴⁰, thus yielding coherent scattering, with the light being subject to the Faraday effect and the atoms evolving by the dynamic Stark effect. The optical output was combined with another optical pulse (modulated by an EOM) at Alice’s station, where a complete Bell measurement was performed using a balanced beamsplitter followed by two sets of polarization homodyne detectors. Conditioned on the outcome, Bob performed spin rotations on the atoms by applying radiofrequency magnetic field pulses (Fig. 4a).

In this way, deterministic and active light-to-matter teleportation was realized⁴⁰ with a fidelity of 58%. All conditions (1)–(5) were achieved, for an input alphabet of coherent states. We note that atomic ensembles have the potential for good quantum memories¹²⁴ with subsecond coherence times and millisecond storage times¹²⁵. This is an important feature for the construction of a scalable quantum network, where teleportation is used to store flying data (optical modes) into stationary media (atomic ensembles).

This experiment was extended to deterministic and active matter-to-matter CV teleportation⁴¹, between two ensembles of $\sim 10^{12}$ room-temperature caesium atoms, by using a four-wave mixing interaction. As before, Bob’s ensemble (B) was subject to a strong driving pulse whose scattering created a co-propagating sideband field (C) entangled with its collective spin. This field reached Alice’s ensemble (A), which was prepared in a coherent state by application of radiofrequency magnetic field pulses. The interaction with A led to a partial mapping of its state onto C, which was then subject to polarization homodyning. Conditioned on the outcome, Bob rotated the spin of B through radiofrequency magnetic field pulses, thus completing the teleportation from A to B with a fidelity of 55%–70%, depending on the size of the input alphabet. This protocol was also used to teleport time-evolving spin states, which makes it the first example of stroboscopic teleportation (Fig. 4b).

Light-to-matter teleportation has also been achieved with DVs by using cold atomic ensembles⁴². This increased the distance and fidelity but made the protocol probabilistic (50% Bell-efficiency) and passive. A polarization qubit has been transported⁴² over a 7 m fibre onto a collective atomic qubit made from two cold ensembles of $\sim 10^6$ rubidium atoms. Teleportation was performed with 78% fidelity, and the output state was stored for 8 μ s. This protocol was extended to matter-to-matter teleportation between two cold ensembles of $\sim 10^8$ rubidium atoms (at 100 μ K) connected by a 150 m spool of optical fibre⁴³. A single collective atomic excitation (spin wave) was teleported between the ensembles with the aid of polarization qubits. Through Raman scattering, Bob’s spin wave qubit (B) was entangled with a photonic qubit (B’) travelling to Alice. Here, Alice’s spin wave qubit (A) was converted into another photonic qubit (A’). Bell detection of A’ and B’ teleported the state of A onto B with 88% fidelity and a storage time of 129 μ s. Note that subsecond storage times are possible with cold atomic ensembles¹²⁶.

Trapped atomic qubits. Deterministic and active qubit teleportation has been realized with trapped ions^{44–46}, with all conditions (1)–(5) being satisfied. Even if distances are very limited owing to the short-range Coulomb interactions, the storage times in these systems are very long. This makes them good quantum memories for using teleportation as a subroutine in quantum computing.

One study⁴⁴ considered three beryllium ions (⁹Be⁺) confined in a segmented linear Paul trap, with an inter-ion spacing of 3 μ m. The qubits were provided by ground-state hyperfine levels, coupled via stimulated Raman transitions. Resonance fluorescence was used for complete Bell detection and, exploiting spin-echo pulses, a fidelity of 78% was achieved. Another study⁴⁵ considered three calcium ions (⁴⁰Ca⁺) in a linear Paul trap, with an inter-ion distance of 5 μ m. An ion qubit was encoded in a superposition of the $S_{1/2}$ ground state and the metastable $D_{5/2}$ state (lifetime ~ 1.16 s) and manipulated by laser pulses tuned to the 729 nm quadrupole transition. Complete Bell detection was performed by observing resonance fluorescence on photomultiplier tubes. Using rephasing spin-echo pulses, this study achieved a fidelity of 75% with storage lifetimes of 10 ms, with later results⁴⁶ achieving a fidelity of 83%.

Increasing the transmission distance beyond micrometres could be achieved using a photonic-matter interface, whereby photonic

qubits are employed as quantum carriers for state mapping and entanglement distribution, although a practical linear-optics implementation would provide incomplete Bell detection. One study⁴⁷ reported the probabilistic teleportation between two ytterbium ions ($^{171}\text{Yb}^+$) with 90% fidelity (Fig. 4c). This method could be used to build a modular quantum network of trapped ions in which long-distance entanglement between atomic qubits is generated at a rate faster than the decoherence rate¹²⁷.

Trapped ions provide long coherence times but their free-space interface may suffer from inefficient photon collection. An alternative solution may come from cavity quantum electrodynamics, where collection efficiencies are enhanced by the strong atom-cavity coupling, albeit at the expense of shorter coherence times. Following this idea, researchers investigated⁴⁸ probabilistic teleportation between two neutral rubidium atoms (^{87}Rb) trapped in two distant optical cavities, with a fidelity of 88% (Fig. 4d).

Solid-state systems. Probabilistic light-to-matter teleportation can be performed between photonic qubits and solid-state quantum memories composed of semiconductor quantum dots (QDs)⁴⁹

or rare-earth-doped crystals⁵⁰. The first experiment⁴⁹ probabilistically teleported a photonic-frequency qubit generated by a neutral QD (that is, a single-photon pulse in a superposition of two frequencies) onto the electron spin of a charged QD separated by 5 m in a different cryostat. A fidelity of 78% was reported for the four equatorial poles of the Bloch sphere (for which $F_{\text{class}} = 3/4$), with the spin coherence time extending to 13 ns using spin-echo pulses (Fig. 5a).

In the second experiment⁵⁰, telecommunications-wavelength polarization qubits were probabilistically teleported onto a single collective excitation of a rare-earth-doped crystal (a neodymium-based quantum memory that stored photons for 50 ns), achieving a fidelity of 89%. One state was teleported over long distance with slightly reduced fidelity, in a relay configuration where the Bell detection was performed at the output of two 12.4-km-long fibre spools (Fig. 5b). This approach is promising for the availability of quantum memories with very long coherence times¹²⁸.

Deterministic and active matter-to-matter teleportation has also been achieved in solid-state devices. In one study⁵¹, researchers considered superconducting transmon qubits separated by 6 mm

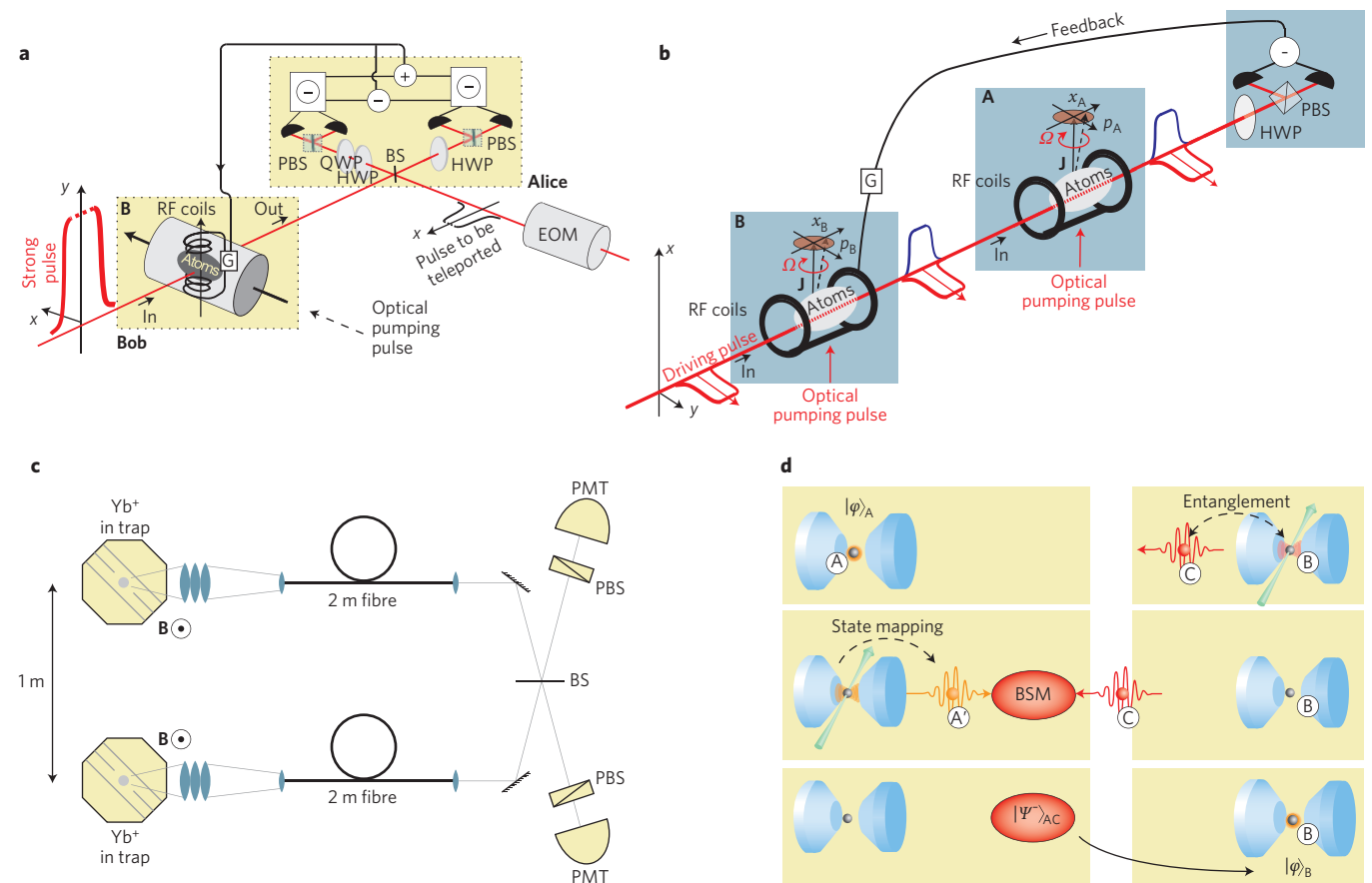


Figure 4 | Quantum teleportation with matter. **a,b**, Teleportation experiments with atomic ensembles of caesium atoms at room temperature, showing light-to-matter teleportation of a coherent state of an optical mode into a collective atomic spin⁴⁰ (**a**) and matter-to-matter teleportation between the collective spins of two atomic ensembles⁴¹ (**b**). RF, radiofrequency. **c,d**, Set-ups with single trapped atoms, where teleportation is achieved by an incomplete Bell detection on emitted photonic qubits. **c**, Teleportation between trapped ytterbium ions, confined in independent Paul traps⁴⁷, 1 m apart and optically connected by a 4 m fibre. Each atomic qubit was encoded in the hyperfine states of the $^2S_{1/2}$ level having coherence times of ~ 2.5 s, and were manipulated by resonant microwave pulses at 12.6 GHz. Spontaneously emitted photons were coupled into fibres and directed to a beamsplitter, where the output ports were filtered in polarization and detected by single-photon photomultiplier tubes (PMTs), implementing a Bell detection with 25% efficiency. **d**, Teleportation between two neutral rubidium atoms (A and B) trapped in optical cavities separated by a 21 m optical fibre⁴⁸. Qubits were encoded in two Zeeman states of the atomic ground-state manifold. Atom-photon entanglement and state mapping were efficiently achieved by vacuum-stimulated Raman adiabatic passage. The generated photonic qubits (A' and C) were then subject to an incomplete Bell detection (25% efficiency). Upon selecting one of the four Bell states $|\Psi\rangle$, the input state $|\varphi\rangle$ was teleported from atom A to atom B. Figures adapted with permission from: **a**, ref. 40, NPG; **b**, ref. 41, NPG; **c**, ref. 47, AAAS; **d**, ref. 48, APS.

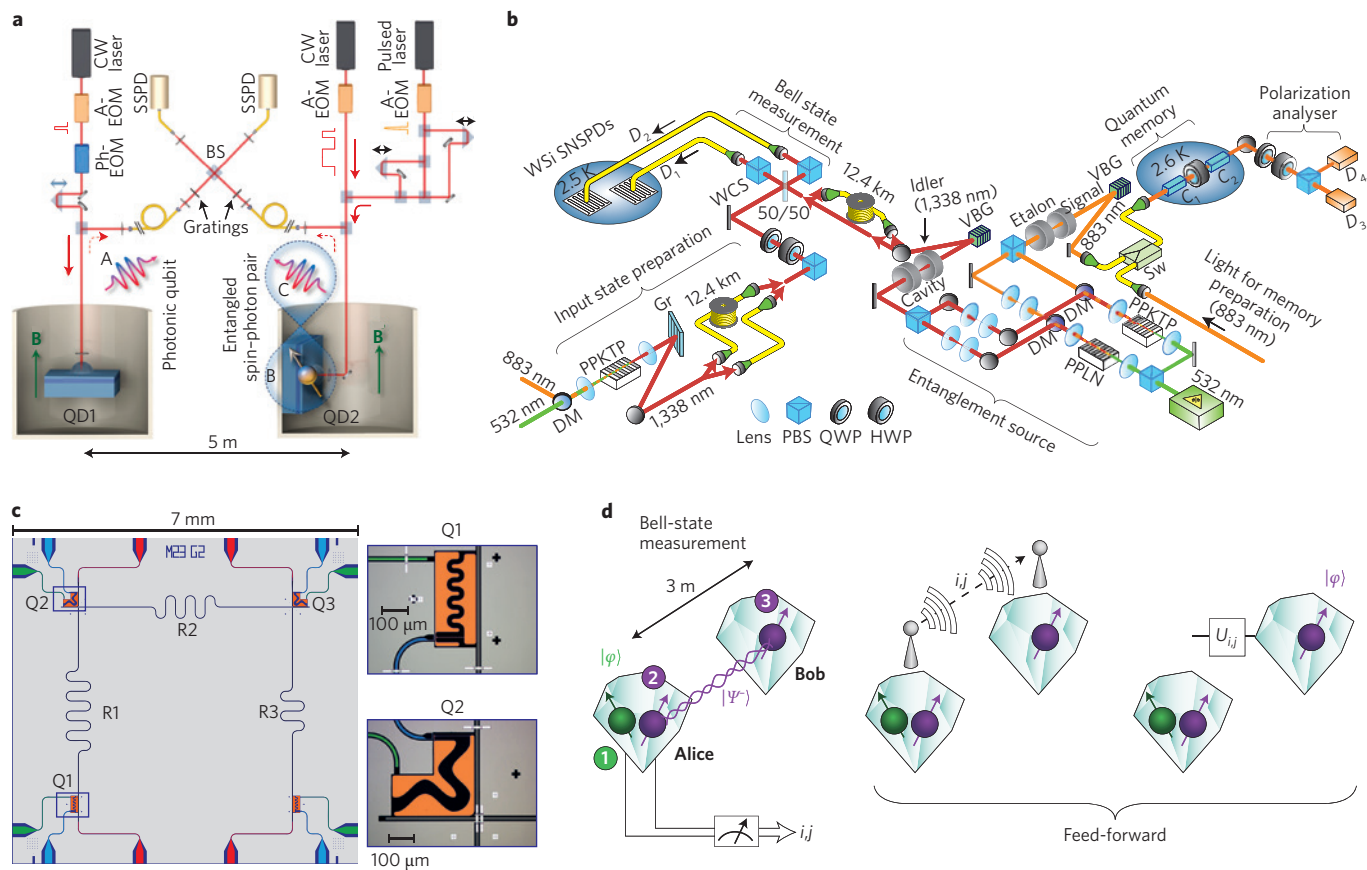


Figure 5 | Quantum teleportation with solid-state systems. **a**, Teleportation of a photonic frequency qubit A, generated by exciting a neutral QD (QD1), onto the electron spin B of a charged QD (QD2)⁴⁹. By means of resonant optical excitation, the spin B was entangled with a second frequency qubit C, sent to interfere with A in a Hong–Ou–Mandel interferometer. A coincidence detection at the output of the interferometer heralded successful photonic-to-spin teleportation with 25% Bell efficiency. A-EOM, amplitude EOM; Ph-EOM, phase EOM; SSPD, superconducting single-photon detector. **b**, Set-up for teleporting a telecommunications polarization qubit onto a rare-earth-doped crystal quantum memory⁵⁰. Two polarization-entangled photons were generated via spontaneous parametric downconversion in nonlinear waveguides, and one of the photons (883 nm) was stored in the quantum memory 10 m away. The other photon (1,338 nm) was sent to interfere with the input polarized photon at the Bell analyser (25% Bell efficiency), where they were measured by superconducting-nanowire single-photon detectors (SNSPD) operating at 2.5 K. Teleportation of the specific state $|+\rangle$ was extended to a total of 24.8 km in coiled fibre. PPKTP, periodically poled potassium titanyl phosphate; Gr, grating; VBG, volume Bragg gratings; Sw, switch; WCS, weak coherent state; PPLN, periodically poled lithium niobate. **c**, Chip design for teleportation between two superconducting transmon qubits, from Q1 to Q3, using the middle qubit Q2 and the two resonators, R1 and R2. The resonators act as quantum buses for entanglement generation and complete Bell detection⁵¹. The qubits were manipulated by applying microwave pulses through individual charge gate lines, and Bell state detection was performed using Josephson parametric amplifiers. **d**, Teleportation between two nitrogen-vacancy centres in diamonds⁵². Once the electronic spins (2 and 3) are entangled, the nitrogen nuclear spin (1) is Bell-detected together with the electronic spin (2) of the same centre. Finally, real-time feed-forward yields teleportation onto the other electron spin (3). Figures adapted with permission from: **a**, ref. 49, NPG; **b**, ref. 50, NPG; **c**, ref. 51, NPG; **d**, ref. 52, AAAS.

and coupled to waveguide resonators in a circuit quantum electrodynamics set-up¹²⁹ (Fig. 5c). The experiment⁵¹ realized probabilistic teleportation (fidelity ~81%) and deterministic teleportation (fidelity ~77%) — also including real-time feed-forward (fidelity ~69%) — at a rate of 10^4 Hz with microsecond coherence times. The set-up employed a quantum bus technology capable of scaling to more complex planar architectures, with non-trivial implications for solid-state quantum computing.

Finally, researchers have also successfully teleported between two diamond nitrogen–vacancy centres separated by 3 m, with complete Bell detection and real-time feed-forward⁵². These centres were addressed by cryogenic confocal microscopes, and their spins were manipulated by spin-resolved optical excitations and microwave pulses. The electronic spins of the centres were entangled through entanglement swapping (coupling them with optical fields that were subsequently overlapped at a beamsplitter and detected). Conditioned upon success of this procedure, the nitrogen nuclear spin of the first centre was prepared and Bell-detected together

with the electronic spin of the same centre. Teleportation onto the electronic spin of the second centre was achieved with an estimated fidelity of 86% (Fig. 5d). Nitrogen–vacancy centres are particularly attractive for combining an optical interface (via the electron spin) with a long-lived nuclear spin memory, having coherence times exceeding 1 s at room temperature¹³⁰.

Discussion and outlook

Table 1 summarizes the optimal experimental performances that are currently achievable using various substrates and techniques. It is clear that there is no single quantum system or technology that excels in all parameters. Still, we may try to identify preferred candidates in relation to specific applications of quantum teleportation. Suitable hybridization of these candidates with compatible substrates and techniques may provide the most promising future developments for quantum teleportation and its applications.

Short-distance teleportation (below 1 m) as a quantum computing subroutine is promising on solid-state devices, with the best

Table 1 | Comparing quantum teleportation technologies.

Quantum technology		Bell efficiency	Fidelity		Maximum distance	Quantum memory
			Passive	Active		
Photonic qubits	Polarization ^{15,16,20,21}	≤50%*	86% ²¹	83% ²¹	143 km ²¹	N/A [†]
	Single-rail qubits ^{22,23}	50%	95% ²²	90% ²³	Table-top	N/A [†]
	Dual-rails in free-space ²⁴	25%	80%	—	Table-top	N/A [†]
	Dual-rails on chip ²⁵	1/27	89%	—	On-chip	N/A [†]
	Time-bins ^{26–28}	25%	81% ^{26‡}	—	6 km fibre ^{27§}	N/A [†]
	Spin-orbital qubits ²⁹	1/32	57–68%	—	Table-top	N/A [†]
NMR ³⁰		100%	—	–90% [¶]	~1 Å	–1 s
Optical modes	CVs ^{31–38}	100%	—	83% ³⁸	12 m ³⁷	N/A [†]
	Hybrid ³⁹	100%	—	79–82%	Table-top	N/A [†]
Atomic ensembles	(Hot) CV light-to-matter ⁴⁰	100%	—	58%	Table-top	4 ms ¹²⁵
	(Hot) CV matter-to-matter ⁴¹	100%	—	55–70%	Table-top (0.5 m)	4 ms ¹²⁵
	(Cold) DV light-to-matter ⁴²	50%	78%	—	7 m fibre	100 ms ¹²⁶
	(Cold) DV matter-to-matter ⁴³	50%	88%	—	150 m fibre [#]	100 ms ¹²⁶
Trapped atoms	Trapped ions ^{44–46}	100%	—	83% ⁴⁶	5 μm ⁴⁵	50 s ^{135**}
	Trapped ions and photonic carriers ⁴⁷	25%	90%	—	4 m fibre ^{††}	50 s ^{135**}
	Neutral atoms in an optical cavity ⁴⁸	25%	88%	—	21 m fibre	184 μs ¹³⁶
Solid state	Frequency qubit to quantum dot ⁴⁹	25%	78% ^{‡‡}	—	5 m	≥1 μs ^{137**}
	Polarization qubit to rare-earth crystal ⁵⁰	25%	89%	—	24.8 km fibre ^{§§}	1 ms ¹³⁸ –6 h ^{128**}
	Superconducting qubits on chip ⁵¹	100%	77%	69%	On-chip (6 mm)	<1 ms ^{139**}
	Nitrogen–vacancy centres in diamonds ⁵²	100%	—	86%	3 m	–0.6 s ¹⁴⁰ ≥1 s ^{130¶¶}

Comparison made in terms of various quality factors, including the practical efficiency of the Bell state analyser, the maximum teleportation fidelity (in active or passive set-ups), the maximum distance of teleportation in free-space (or fibre, where indicated), and the storage time of associated quantum memories. The storage time can be either the typical decay time of the stored qubit (estimated from the retrieval efficiency of the memory) or the time needed for the write-read fidelity to drop below the classical threshold value (for example, this is the definition used for CVs). In some cases, we show the maximum coherence time, which typically involves the use of dynamical decoupling techniques. Symbols: *Excluding set-ups with internal qubit preparation^{17,18}; †Optical delays based on fibres or cavities that have very short storage times; †Fidelity of 93% was achieved for the four equatorial states²⁸; ‡Coiled fibre, Alice–Bob flight distance –55 m (extended to 550 m in ref. 28); ††Two-qubit teleportation with classical fidelity of 40%; ¶Entanglement fidelity³⁰; #Coiled fibre, Alice–Bob flight distance –0.6 m; **Maximum coherence time; †††Alice–Bob flight distance –1 m; ††††Equatorial states teleported; †††††One state teleported over 24.8 km of coiled fibre with 81% fidelity (Alice–Bob flight distance –10 m); ††††††Coherence time for electronic spins at low temperatures (–77 K); †††††††Coherence time for nuclear spins at room temperature.

approach being circuit quantum electrodynamics¹²⁹. In particular, superconducting transmon qubits may guarantee both deterministic and high-fidelity teleportation on chip⁵¹. They also allow the implementation of real-time feed-forward, which seems to be more challenging with photonic chips²⁵. Moreover, compared with earlier approaches such as trapped ions, they provide a more scalable architecture and better integration with existing technology. The current downside of these systems seems to be their limited coherence time (below 1 ms). This problem can be overcome by integrating circuit quantum electrodynamics with solid-state spin-ensemble quantum memories (nitrogen–vacancy centres or rare-earth-doped crystals), which can provide very long coherence times for quantum data storage. This is currently one of the biggest efforts across the community^{131,132}.

Teleportation-empowered quantum communication at the metropolitan scale (a few kilometres) could be developed using optical modes^{31,38}. For sufficiently low loss, these systems provide high rates and bandwidths (for instance, see the high-rate performances achievable in CV quantum key distribution⁸⁷). Experiments may be extended from table-top to medium-range implementations, in fibre or free-space, and to consider potential integration with ensemble-based quantum memories. Longer distances at lower rates may be achieved via a hybrid approach³⁹ or by developing good quantum repeaters based on non-Gaussian operations⁸⁵.

Research into long-distance quantum teleportation (beyond 100 km) is active but still affected by an unsolved problem. Although polarization qubits are the best carriers for (low-rate) teleportation over long fibres and free-space links, they currently make the protocol probabilistic owing to the incomplete Bell detection.

Although probabilistic teleportation and entanglement swapping are acceptable for tasks such as entanglement distillation and quantum cryptography⁸⁶, the situation is clearly different for quantum communication, where the input quantum information must be fully preserved.

Thus, provided one is willing to work within the limitations imposed by probabilistic protocols, then satellite-based implementations are within the reach of current technology. Besides the integration of tracking techniques, the main challenge is to overcome the high losses associated with beam spreading. This could be achieved in a configuration where entanglement is distributed from a satellite to large-aperture ground-station telescopes. Assuming 1 m aperture telescopes and a 20 cm aperture satellite at an altitude of ~600 km, one can estimate a loss of ~75 dB for a two-downlink channel, which is less than the ~80 dB loss achieved at ground level for entanglement distribution²⁰. Ground-to-satellite or inter-satellite implementations are more challenging.

The future use of quantum teleportation as a building block in scalable quantum networks depends on its integration with quantum memories. Such memories must come with excellent radiation–matter interfaces, in terms of conversion efficiency, write–read fidelity, storage time and bandwidth (high rate and storage capacity)¹²⁴. The development of good quantum memories would enable not only the distribution of entanglement across a network (via quantum repeaters) and quantum communication via teleportation, but also the ability to store and process the transmitted quantum information. This could ultimately transform the network into a world-wide distributed quantum computer or backbone for a future quantum internet¹³.

From this point of view, atomic ensembles are traditionally considered appealing for their efficient light-to-matter conversion¹²⁴ and their millisecond storage times, which can approach the ~100 ms required by light for transmission on a global scale. However, very promising developments are also coming from solid-state systems, where excellent spin-ensemble quantum memories offer direct integration with the scalable architecture of circuit quantum electrodynamics. These memories may not only extend the coherence time of circuit quantum electrodynamics, but also provide an optical–microwave interface for inter-converting propagating optical/telecommunications photons with on-chip microwave photons^{132,133}. Thus, a revised hybrid architecture for the future quantum internet could be based on solid-state nodes (for local quantum information processing) suitably connected by long-distance quantum optical communication, which may be exploited for inter-node quantum teleportation.

Received 3 June 2014; accepted 23 July 2015;
published online 29 September 2015

References

- Fort, C. H. *Lo!* (Claude Kendall, 1931).
- Bennett, C. H. *et al.* Teleporting an unknown quantum state via dual classical and Einstein-Podolsky-Rosen channels. *Phys. Rev. Lett.* **70**, 1895–1899 (1993).
- Horodecki, R., Horodecki, P., Horodecki, M. & Horodecki, K. Quantum entanglement. *Rev. Mod. Phys.* **81**, 865–942 (2009).
- Eisert, J. & Plenio, M. B. Introduction to the basics of entanglement theory in continuous-variable systems. *Int. J. Quant. Inf.* **1**, 479–506 (2003).
- Nielsen, M. A. & Chuang, I. L. *Quantum Computation and Quantum Information* (Cambridge Univ., 2000).
- Wilde, M. M. *Quantum Information Theory* (Cambridge Univ. Press, 2013).
- Weedbrook, C. *et al.* Gaussian quantum information. *Rev. Mod. Phys.* **84**, 621–669 (2012).
- Braunstein, S. L. & van Loock, P. Quantum information theory with continuous variables. *Rev. Mod. Phys.* **77**, 513–577 (2005).
- Briegel, H.-J., Dür, W., Cirac, J. I. & Zoller, P. Quantum repeaters: The role of imperfect local operations in quantum communication. *Phys. Rev. Lett.* **81**, 5932–5935 (1998).
- Gottesman, D. & Chuang, I. L. Demonstrating the viability of universal quantum computation using teleportation and single-qubit operations. *Nature* **402**, 390–393 (1999).
- Raussendorf, R. & Briegel, H. J. A one-way quantum computer. *Phys. Rev. Lett.* **86**, 5188–5191 (2001).
- Ishizaka, S. & Hiroshima, T. Asymptotic teleportation scheme as a universal programmable quantum processor. *Phys. Rev. Lett.* **101**, 240501 (2008).
- Kimble, H. J. The quantum internet. *Nature* **453**, 1023–1030 (2008).
- Lloyd, S. *et al.* Closed timelike curves via post-selection: theory and experimental demonstration. *Phys. Rev. Lett.* **106**, 040403 (2011).
- Bouwmeester, D. *et al.* Experimental quantum teleportation. *Nature* **390**, 575–579 (1997).
- Ursin, R. *et al.* Quantum teleportation across the Danube. *Nature* **430**, 849 (2004).
- Boschi, D., Branca, S., De Martini, F., Hardy, L. & Popescu, S. Experimental realisation of teleporting an unknown pure quantum state via dual classical and Einstein-Podolski-Rosen channels. *Phys. Rev. Lett.* **80**, 1121–1125 (1998).
- Jin, X.-M. *et al.* Experimental free-space quantum teleportation. *Nature Photon.* **4**, 376–381 (2010).
- Kim, Y.-H., Kulik, S. P. & Shih, Y. Quantum teleportation of a polarisation state with complete Bell state measurement. *Phys. Rev. Lett.* **86**, 1370–1373 (2001).
- Yin, J. *et al.* Quantum teleportation and entanglement distribution over 100-kilometre free-space channels. *Nature* **488**, 185–188 (2012).
- Ma, X.-S. *et al.* Quantum teleportation over 143 kilometres using active feed-forward. *Nature* **489**, 269–273 (2012).
- Lombardi, E., Sciarrino, F., Popescu, S. & De Martini, F. Teleportation of a vacuum-one-photon qubit. *Phys. Rev. Lett.* **88**, 070402 (2002).
- Giacomini, S., Sciarrino, F., Lombardi, E. & De Martini, F. Active teleportation of a quantum bit. *Phys. Rev. A* **66**, 030302 (2002).
- Fattal, D., Diamanti, E., Inoue, K. & Yamamoto, Y. Quantum teleportation with a quantum dot single photon source. *Phys. Rev. Lett.* **92**, 037904 (2004).
- Metcalfe, B. J. *et al.* Quantum teleportation on a photonic chip. *Nature Photon.* **8**, 770–774 (2014).
- Marcikic, I., de Riedmatten, H., Tittel, W., Zbinden, H. & Gisin, N. Long-distance teleportation of qubits at telecommunication wavelengths. *Nature* **421**, 509–513 (2003).
- de Riedmatten, H. *et al.* Long distance quantum teleportation in a quantum relay configuration. *Phys. Rev. Lett.* **92**, 047904 (2004).
- Landry, O. *et al.* Quantum teleportation over the Swisscom telecommunication network. *J. Opt. Soc. Am. B* **24**, 398–403 (2007).
- Wang, X.-L. *et al.* Quantum teleportation of multiple degrees of freedom in a single photon. *Nature* **518**, 516–519 (2015).
- Nielsen, M. A., Knill, E. & Laflamme, R. Complete quantum teleportation using nuclear magnetic resonance. *Nature* **396**, 52–55 (1998).
- Furusawa, A. *et al.* Unconditional quantum teleportation. *Science* **282**, 706–709 (1998).
- Bowen, W. P. *et al.* Experimental investigation of continuous-variable quantum teleportation. *Phys. Rev. A* **67**, 032302 (2003).
- Zhang, T. C., Goh, K. W., Chou, C. W., Lodahl, P. & Kimble, H. J. Quantum teleportation of light beams. *Phys. Rev. A* **67**, 033802 (2003).
- Takei, N., Yonezawa, H., Aoki, T. & Furusawa, A. High-fidelity teleportation beyond the no-cloning limit and entanglement swapping for continuous variables. *Phys. Rev. Lett.* **94**, 220502 (2005).
- Yonezawa, H., Braunstein, S. L. & Furusawa, A. Experimental demonstration of quantum teleportation of broadband squeezing. *Phys. Rev. Lett.* **99**, 110503 (2007).
- Takei, N. *et al.* Experimental demonstration of quantum teleportation of a squeezed state. *Phys. Rev. A* **72**, 042304 (2005).
- Lee, N. *et al.* Teleportation of nonclassical wave packets of light. *Science* **332**, 330–333 (2011).
- Yukawa, M., Benichi, H. & Furusawa, A. High-fidelity continuous-variable quantum teleportation toward multistep quantum operations. *Phys. Rev. A* **77**, 022314 (2008).
- Takeda, S., Mizuta, T., Fuwa, M., van Loock, P. & Furusawa, A. Deterministic quantum teleportation of photonic quantum bits by a hybrid technique. *Nature* **500**, 315–318 (2013).
- Sherson, J. F. *et al.* Quantum teleportation between light and matter. *Nature* **443**, 557–560 (2006).
- Krauter, H. *et al.* Deterministic quantum teleportation between distant atomic objects. *Nature Phys.* **9**, 400–404 (2013).
- Chen, Y.-A. *et al.* Memory-built-in quantum teleportation with photonic and atomic qubits. *Nature Phys.* **4**, 103–107 (2008).
- Bao, X.-H. *et al.* Quantum teleportation between remote atomic-ensemble quantum memories. *Proc. Natl Acad. Sci. USA* **109**, 20347–20351 (2012).
- Barrett, M. D. *et al.* Deterministic quantum teleportation of atomic qubits. *Nature* **429**, 737–739 (2004).
- Riebe, M. *et al.* Deterministic quantum teleportation with atoms. *Nature* **429**, 734–737 (2004).
- Riebe, M. *et al.* Quantum teleportation with atoms: Quantum process tomography. *New J. Phys.* **9**, 211 (2007).
- Olmschenk, S. *et al.* Quantum teleportation between distant matter qubits. *Science* **323**, 486–489 (2009).
- Nölleke, C. *et al.* Efficient teleportation between remote single-atom quantum memories. *Phys. Rev. Lett.* **110**, 140403 (2013).
- Gao, W. B. *et al.* Quantum teleportation from a propagating photon to a solid-state spin qubit. *Nature Commun.* **4**, 2744 (2013).
- Bussi eres, F. *et al.* Quantum teleportation from a telecom-wavelength photon to a solid-state quantum memory. *Nature Photon.* **8**, 775–778 (2014).
- Steffen, L. *et al.* Deterministic quantum teleportation with feed-forward in a solid state system. *Nature* **500**, 319–322 (2013).
- Pfaff, W. *et al.* Unconditional quantum teleportation between distant solid-state quantum bits. *Science* **345**, 532–535 (2014).
- Weinfurter, H. Experimental Bell-state analysis. *Europhys. Lett.* **25**, 559–564 (1994).
- Braunstein, S. L. & Mann, A. Measurement of the Bell operator and quantum teleportation. *Phys. Rev. A* **51**, R1727–R1730 (1995).
- Calsamiglia, J. & L utkenhaus, N. Maximum efficiency of a linear-optical Bell-state analyzer. *Appl. Phys. B* **72**, 67–71 (2001).
- Bennett, C. H. *et al.* Remote state preparation. *Phys. Rev. Lett.* **87**, 077902 (2001).
- Scarani, V., Iblisdir, S., Gisin, N. & Acn, A. Quantum cloning. *Rev. Mod. Phys.* **77**, 1225–1256 (2005).
- Massar, S. & Popescu, S. Optimal extraction of information from finite quantum ensembles. *Phys. Rev. Lett.* **74**, 1259–1263 (1995).
- Werner, R. F. All teleportation and dense coding schemes. *J. Phys. A* **34**, 7081–7094 (2001).
- Vaidman, L. Teleportation of quantum states. *Phys. Rev. A* **49**, 1473–1476 (1994).
- Braunstein, S. L. & Kimble, H. J. Teleportation of continuous quantum variables. *Phys. Rev. Lett.* **80**, 869–872 (1998).

62. Pirandola, S., Mancini, S., Vitali, D. & Tombesi, P. Continuous variable entanglement and quantum state teleportation between optical and macroscopic vibrational modes through radiation pressure. *Phys. Rev. A* **68**, 062317 (2003).
63. Eisert, J. *Entanglement in quantum information theory*. PhD thesis, Potsdam University (2001).
64. Vidal, G. & Werner, R. F. Computable measure of entanglement. *Phys. Rev. A* **65**, 032314 (2002).
65. Plenio, M. B. Logarithmic negativity: A full entanglement monotone that is not convex. *Phys. Rev. Lett.* **95**, 090503 (2005).
66. Walls, D. F. & Milburn, G. J. *Quantum Optics* (Springer, 1994).
67. Braunstein, S. L., Fuchs, C. A., Kimble, H. J. & van Loock, P. Quantum versus classical domains for teleportation with continuous variables. *Phys. Rev. A* **64**, 022321 (2001).
68. Hammerer, K., Wolf, M. M., Polzik, E. S. & Cirac, J. I. Quantum benchmark for storage and transmission of coherent states. *Phys. Rev. Lett.* **94**, 150503 (2005).
69. Grosshans, F. & Grangier, P. Quantum cloning and teleportation criteria for continuous quantum variables. *Phys. Rev. A* **64**, 010301(R) (2001).
70. Pirandola, S. & Mancini, S. Quantum teleportation with continuous variables: A survey. *Laser Phys.* **16**, 1418–1438 (2006).
71. Hammerer, K., Wolf, M. M., Polzik, E. S. & Cirac, J. I. Quantum benchmark for storage and transmission of coherent states. *Phys. Rev. Lett.* **94**, 150503 (2005).
72. Owari, M., Plenio, M. B., Polzik, E. S., Serafini, A. & Wolf, M. M. Squeezing the limit: Quantum benchmarks for the teleportation and storage of squeezed states. *New J. Phys.* **10**, 113014 (2008).
73. Calsamiglia, J., Aspachs, M., Muñoz Tapia, R. & Bagan, E. Phase-covariant quantum benchmarks. *Phys. Rev. A* **79**, 050301(R) (2009).
74. Chiribella, G. & Adesso, G. Quantum benchmarks for pure single-mode Gaussian states. *Phys. Rev. Lett.* **112**, 010501 (2014).
75. van Loock, P., Braunstein, S. L. & Kimble, H. J. Broadband teleportation. *Phys. Rev. A* **62**, 022309 (2000).
76. Zukowski, M., Zeilinger, A., Horne, M. A. & Ekert, A. “Event-ready-detectors” Bell experiment via entanglement swapping. *Phys. Rev. Lett.* **71**, 4287–4290 (1993).
77. Pan, J.-W., Bouwmeester, D., Weinfurter, H. & Zeilinger, A. Experimental entanglement swapping: Entangling photons that never interacted. *Phys. Rev. Lett.* **80**, 3891–3894 (1998).
78. van Loock, P. & Braunstein, S. L. Unconditional teleportation of continuous-variable entanglement. *Phys. Rev. A* **61**, 010302(R) (1999).
79. Polkinghorne, R. E. S. & Ralph, T. C. Continuous variable entanglement swapping. *Phys. Rev. Lett.* **83**, 2095–2099 (1999).
80. Pirandola, S., Vitali, D., Tombesi, P. & Lloyd, S. Macroscopic entanglement by entanglement swapping. *Phys. Rev. Lett.* **97**, 150403 (2006).
81. Abdi, M., Pirandola, S., Tombesi, P. & Vitali, D. Entanglement swapping with local certification: Application to remote micromechanical resonators. *Phys. Rev. Lett.* **109**, 143601 (2012).
82. Jia, X. *et al.* Experimental demonstration of unconditional entanglement swapping for continuous variables. *Phys. Rev. Lett.* **93**, 250503 (2004).
83. Takeda, S., Fuwa, M., van Loock, P. & Furusawa, A. Entanglement swapping between discrete and continuous variables. *Phys. Rev. Lett.* **114**, 100501 (2015).
84. Bennett, C. H. *et al.* Purification of noisy entanglement and faithful teleportation via noisy channels. *Phys. Rev. Lett.* **76**, 722–725 (1996).
85. Eisert, J., Browne, D. E., Scheel, S. & Plenio, M. B. Distillation of continuous-variable entanglement with optical means. *Ann. Phys.* **311**, 431–458 (2004).
86. Braunstein, S. L. & Pirandola, S. Side-channel-free quantum key distribution. *Phys. Rev. Lett.* **108**, 130502 (2012).
87. Pirandola, S. *et al.* High-rate measurement-device-independent quantum cryptography. *Nature Photon.* **9**, 397–402 (2015).
88. Karlsson, A. & Bourennane, M. Quantum teleportation using three-particle entanglement. *Phys. Rev. A* **58**, 4394–4400 (1998).
89. Hillery, M., Buzek, V. & Berthiaume, A. Quantum secret sharing. *Phys. Rev. A* **59**, 1829–1834 (1999).
90. van Loock, P. & Braunstein, S. L. Multipartite entanglement for continuous variables: A quantum teleportation network. *Phys. Rev. Lett.* **84**, 3482–3485 (2000).
91. Yonezawa, H., Aoki, T. & Furusawa, A. Demonstration of a quantum teleportation network for continuous variables. *Nature* **431**, 430–433 (2004).
92. Lance, A. M., Symul, T., Bowen, W. P., Sanders, B. C. & Lam, P. K. Tripartite quantum state sharing. *Phys. Rev. Lett.* **92**, 177903 (2004).
93. Bužek, V. & Hillery, M. Quantum copying: Beyond the no-cloning theorem. *Phys. Rev. A* **54**, 1844–1852 (1996).
94. Bruß, D. *et al.* Optimal universal and state-dependent quantum cloning. *Phys. Rev. A* **57**, 2368–2378 (1998).
95. Cerf, N. J., Ipe, A. & Rottenberg, X. Cloning of continuous quantum variables. *Phys. Rev. Lett.* **85**, 1754–1757 (2000).
96. Zhao, Z. *et al.* Experimental realisation of optimal asymmetric cloning and telecloning via partial teleportation. *Phys. Rev. Lett.* **95**, 030502 (2005).
97. Koike, S. *et al.* Demonstration of quantum telecloning of optical coherent states. *Phys. Rev. Lett.* **96**, 060504 (2006).
98. Murao, M., Jonathan, D., Plenio, M. B. & Vedral, V. Quantum telecloning and multiparticle entanglement. *Phys. Rev. A* **59**, 156–161 (1999).
99. van Loock, P. & Braunstein, S. L. Telecloning of continuous quantum variables. *Phys. Rev. Lett.* **87**, 247901 (2001).
100. Brassard, G., Braunstein, S. L. & Cleve, R. Teleportation as a quantum computation. *Physica D* **120**, 43–47 (1998).
101. Aliferis, P. & Leung, D. W. Computation by measurements: A unifying picture. *Phys. Rev. Lett.* **70**, 062314 (2004).
102. Knill, E., Laflamme, R. & Milburn, G. A scheme for efficient quantum computation with linear optics. *Nature* **409**, 46–52 (2001).
103. Gao, W.-B. *et al.* Teleportation-based realisation of an optical quantum two-qubit entangling gate. *Proc. Natl Acad. Sci. USA* **107**, 20869–20874 (2010).
104. Gross, D. & Eisert, J. Novel schemes for measurement-based quantum computing. *Phys. Rev. Lett.* **98**, 220503 (2007).
105. Nielsen, M. A. Optical quantum computation using cluster states. *Phys. Rev. Lett.* **93**, 040503 (2004).
106. Menicucci, N. C. *et al.* Universal quantum computation with continuous-variable cluster states. *Phys. Rev. Lett.* **97**, 110501 (2006).
107. Zhang, J. & Braunstein, S. L. Continuous-variable Gaussian analog of cluster states. *Phys. Rev. A* **73**, 032318 (2006).
108. Yokoyama, S. *et al.* Ultra-large-scale continuous-variable cluster states multiplexed in the time domain. *Nature Photon.* **7**, 982–986 (2013).
109. Ishizaka, S. & Hiroshima, T. Quantum teleportation scheme by selecting one of multiple output ports. *Phys. Rev. A* **79**, 042306 (2009).
110. Strelchuk, S., Horodecki, M. & Oppenheim, J. Generalised teleportation and entanglement recycling. *Phys. Rev. Lett.* **110**, 010505 (2013).
111. Beigi, S. & König, R. Simplified instantaneous non-local quantum computation with applications to position-based cryptography. *New J. Phys.* **13**, 093036 (2011).
112. Buhrman, H. *et al.* Quantum communication complexity advantage implies violation of a Bell inequality. Preprint at <http://arxiv.org/abs/1502.01058v1> (2015).
113. Grice, W. P. Arbitrarily complete Bell-state measurement using only linear optical elements. *Phys. Rev. A* **84**, 042331 (2011).
114. Zaidi, H. A. & van Loock, P. Beating the one-half limit of ancilla-free linear optics Bell measurements. *Phys. Rev. Lett.* **110**, 260501 (2013).
115. Ewert, F. & van Loock, P. 3/4-efficient Bell measurement with passive linear optics and unentangled ancillae. *Phys. Rev. Lett.* **113**, 140403 (2014).
116. Braunstein, S. L. & Kimble, H. J. *A posteriori* teleportation. *Nature* **394**, 840–841 (1998).
117. Pan, J.-W., Gasparoni, S., Aspelmeyer, M., Jennewein, T. & Zeilinger, A. Experimental realization of freely propagating teleported qubits. *Nature* **421**, 721–725 (2003).
118. Lee, H.-W. & Kim, J. Quantum teleportation and Bell’s inequality using single-particle entanglement. *Phys. Rev. A* **63**, 012305 (2000).
119. Brendel, J., Tittel, W., Zbinden, H. & Gisin, N. Pulsed energy-time entangled twin-photon source for quantum communication. *Phys. Rev. Lett.* **82**, 2594–2597 (1999).
120. Ou, Z. Y., Pereira, S. F., Kimble, H. J. & Peng, K. C. Realization of the Einstein–Podolsky–Rosen paradox for continuous variables. *Phys. Rev. Lett.* **68**, 3663–3666 (1992).
121. Schori, C., Sørensen, J. L. & Polzik, E. S. Narrow-band frequency tunable light source of continuous quadrature entanglement. *Phys. Rev. A* **66**, 033802 (2002).
122. Furusawa, A. & van Loock, P. *Quantum Teleportation and Entanglement — A Hybrid Approach to Optical Quantum Information Processing* (Wiley, 2011).
123. Andersen, U. L. & Ralph, T. C. High-fidelity teleportation of continuous-variable quantum states using delocalised single photons. *Phys. Rev. Lett.* **111**, 050504 (2013).
124. Simon, C. *et al.* Quantum memories. *Eur. Phys. J. D* **58**, 1–22 (2010).
125. Julsgaard, B. *et al.* Experimental demonstration of quantum memory for light. *Nature* **432**, 482–486 (2004).
126. Radnaev, A. G. *et al.* A quantum memory with telecom-wavelength conversion. *Nature Phys.* **6**, 894–899 (2010).
127. Hucul, D. *et al.* Modular entanglement of atomic qubits using photons and phonons. *Nature Phys.* **11**, 37–42 (2015).
128. Zhong, M. *et al.* Optically addressable nuclear spins in a solid with a six-hour coherence time. *Nature* **517**, 177–180 (2015).
129. Schoelkopf, R. J. & Girvin, S. M. Wiring up quantum systems. *Nature* **451**, 664–669 (2008).
130. Maurer, P. C. *et al.* Room-temperature quantum bit memory exceeding one second. *Science* **336**, 1283–1286 (2012).

131. Xiang, Z.-L., Ashhab, S., You, J. Q. & Nori, F. Hybrid quantum circuits: Superconducting circuits interacting with other quantum systems. *Rev. Mod. Phys.* **85**, 623–653 (2013).
132. Kurizki, G. *et al.* Quantum technologies with hybrid systems. *Proc. Natl Acad. Sci. USA* **112**, 3866–3873 (2015).
133. O'Brien, C., Lauk, N., Blum, S., Morigi, G. & Fleischhauer, M. Interfacing superconducting qubits and telecom photons via a rare-earth-doped crystal. *Phys. Rev. Lett.* **113**, 063603 (2014).
134. Braunstein, S. L., D'Ariano, G. M., Milburn, G. J. & Sacchi, M. F. Universal teleportation with a twist. *Phys. Rev. Lett.* **84**, 3486–3489 (2000).
135. Harty, T. P. *et al.* High-fidelity preparation, gates, memory, and readout of a trapped-ion quantum bit. *Phys. Rev. Lett.* **113**, 220501 (2014).
136. Specht, H. P. *et al.* A single-atom quantum memory. *Nature* **473**, 190–193 (2011).
137. Press, D. *et al.* Ultrafast optical spin echo in a single quantum dot. *Nature Photon.* **4**, 367–370 (2010).
138. Jobez, P. *et al.* Coherent spin control at the quantum level in an ensemble-based optical memory. *Phys. Rev. Lett.* **114**, 230502 (2015).
139. Reagor, M. *et al.* A quantum memory with near-millisecond coherence in circuit QED. Preprint at <http://arxiv.org/abs/1508.05882> (2015).
140. Bar-Gill, N., Pham, L. M., Jarmola, A., Budker, D. & Walsworth, R. L. Solid-state electronic spin coherence time approaching one second. *Nature Commun.* **4**, 1743 (2013).

Acknowledgements

S.P. was supported by the Leverhulme Trust (qBIO) and the EPSRC, via qDATA (Grant No. EP/L011298/1) and the UK Quantum Communications Hub (Grant No. EP/M013472/1). J.E. was supported by BMBF (Q.com), the EU (SIQS, RAQUEL, AQuS) and the ERC (TAQ). The authors would like to acknowledge useful feedback from U. L. Andersen, G. Chiribella, N. Gisin, A. Imamoglu, C.-Y. Lu, P. van Loock, S. Mancini, C. Monroe, S. Olmschenk, J. W. Pan, W. Pfaff, E. Polzik, S. Popescu, T. C. Ralph, V. Scarani, F. Sciarrino, C. Simon, R. Thew, W. Tittel, A. Wallraff and D. J. Wineland.

Author contributions

All authors contributed to selecting the literature, critical discussions and checking the manuscript for accuracy. S.P. reviewed the selected literature, and wrote the majority of the manuscript. J.E. and S.L.B. contributed to the writing/editing of the theory sections.

Additional information

Reprints and permissions information is available online at www.nature.com/reprints. Correspondence should be addressed to S.P.

Competing financial interests

The authors declare no competing financial interests.